Mon. Not. R. Astron. Soc. **000**, 1–13 (2013) Printed 19 August 2013 (MN LaTeX style file v2.2)

UV-excess sources with a red/IR-counterpart: low-mass companions, debris disks and QSO selection

Kars Verbeek[1⋆], Paul J. Groot[1], Simone Scaringi[1,2], Jorge Casares[3], Jesus M. Corral-Santana[3,4] Niall Deacon[5] Janet E. Drew[6], Boris T. Gänsicke[7], Eduardo González-Solares[8], Robert Greimel[9], Ulrich Heber[10], Ralf Napiwotzki[6], Roy H. Østensen[2], Danny Steeghs[7], Nicholas J. Wright[6] and Albert Zijlstra[11]

[1] *Department of Astrophysics, Radboud University Nijmegen, P.O. Box 9010, 6500 GL Nijmegen, The Netherlands*
[2] *Instituut voor Sterrenkunde, KU Leuven, Celestijnenlaan 200D, B-3001 Leuven, Belgium*
[3] *Instituto de Astrofísica de Canarias, Via Lactea, s/n E-38205 La Laguna (Tenerife), Spain*
[4] *Departamento de Astrofísica, Universidad de La Laguna, La Laguna E-38205, S/C de Tenerife, Spain*
[5] *Max-Planck-Institute für Astronomie, Königstuhl 17, 69117, Heidelberg, Germany*
[6] *Centre for Astronomy Research, Science & Technology Research Institute, University of Hertfordshire, Hatfield, AL10 9AB, UK*
[7] *Physics Department, University of Warwick, Coventry, CV4 7AL, UK*
[8] *Cambridge Astronomy Survey Unit, Institute of Astronomy, University of Cambridge, Madingley Road, Cambridge, CB3 0HA, UK*
[9] *Institut für Physik, Karl-Franzen Universität Graz, Universitätsplatz 5, 8010 Graz, Austria*
[10] *Dr. Remeis-Sternwarte Bamberg, Universität Erlangen-Nürnberg, Sternwartstrasse 7, D-96049 Bamberg, Germany*
[11] *Jodrell Bank Centre for Astrophysics, Alan Turing Building, University of Manchester, M13 9PL, UK*

Accepted for publication in MNRAS

ABSTRACT

We present the result of the cross-matching between UV-excess sources selected from the UV-excess survey of the Northern Galactic Plane (*UVEX*) and several infrared surveys (2*MASS* , *UKIDSS* and *WISE*). From the position in the $(J-H)$ vs. $(H-K)$ colour-colour diagram we select UV-excess candidate white dwarfs with an M-dwarf type companion, candidates that might have a lower mass, brown-dwarf type companion, and candidates showing an infrared-excess only in the K-band, which might be due to a debris disk. Grids of reddened DA+dM and sdO+MS/sdB+MS model spectra are fitted to the U, g, r, i, z, J, H, K photometry in order to determine spectral types and estimate temperatures and reddening. From a sample of 964 hot candidate white dwarfs with $(g-r)$ <0.2, the spectral energy distribution fitting shows that ∼2-4% of the white dwarfs have an M-dwarf companion, ∼2% have a lower-mass companion, and no clear candidates for having a debris disk are found. Additionally, from *WISE* 6 UV-excess sources are selected as candidate Quasi-Stellar Objects (QSOs). Two UV-excess sources have a *WISE* IR-excess showing up only in the mid-IR $W3$ band of *WISE* , making them candidate Luminous InfraRed Galaxies (LIRGs) or Sbc star-burst galaxies.

Key words: surveys – stars: white dwarfs – stars: binaries – ISM:general – Galaxy: stellar content – infrared: stars

1 INTRODUCTION

One of the main goals of the European Galactic Plane Surveys (*EGAPS*) is to obtain a homogeneous sample of evolved objects in our Milky Way with well-known selection limits. The *EGAPS* data also contains more esoteric objects (e.g. Nova V458 Vul, Wesson et al., 2008; Necklace Nebula, Corradi et al., 2011; photo-evaporating prolyd-like objects, Wright et al., 2012). Over the last years the data of large sky surveys yielded several known white dwarfs with gas or dust disks (Gänsicke et al., 2007; Gänsicke et al., 2011; Gänsicke et al., 2008; Zuckerman and Becklin, 1987; Brinkworth et al., 2009; Brinkworth et al., 2012; Kilic et al., 2012; Debes et al., 2011). When optical surveys are cross-matched with the data of infrared (IR) surveys (e.g. *SDSS* -*UKIDSS* : Silvestri et al., 2006; Heller et al.,

⋆ E-mail:k.verbeek@astro.ru.nl

2009; Girven et al., 2011, *SDSS -WISE* : Debes et al., 2011; Hoard et al., 2011, *SDSS -2MASS* : Hoard et al., 2007 and *IPHAS -2MASS* : Wright et al., 2008), the classification of sources can be extended, and hot white dwarfs with companions or debris disks, and other peculiar objects are detected. The dusty debris disks around white dwarfs are believed to form during the destruction of asteroids, the remnants of the planetary systems that orbited the star earlier in its evolution at the main-sequence. Emission lines in the spectra of the white dwarfs indicates that there might also be gaseous material present in these disks. This might also clarify the spectra of metal-polluted white dwarfs (Gänsicke et al., 2012; Debes, Walsh & Stark, 2012; Dufour et al., 2012; Farihi et al., 2012; Debes & Sigurdsson, 2002; Jura, 2003). The time for metals to sink out of the atmosphere of the white dwarf is in the order of a few days for hot DA white dwarfs, and up to 10^6 years for DB/DC white dwarfs (Table 4 to 6 of Koester, 2009; Koester & Wilken, 2006), indicating that accretion is ongoing for most objects. An unknown fraction of the *UVEX* white dwarfs will have an M-dwarf companion (Silvestri et al., 2006; Farihi, Becklin & Zuckerman, 2005; Debes, 2011). From the cross-matching between infrared and optical observations, about 0.2-2% of the white dwarfs are expected to have an IR-excess due to a brown dwarf type companion, and 0.3-4% of the white dwarfs are expected to be debris disk candidates (Girven et al., 2011; Steele et al., 2011; Debes et al., 2011; Barber et al., 2012; Farihi, Becklin & Zuckerman, 2005).

A number of the optically selected UV-excess sources from *UVEX* , as described in Verbeek et al. (2012a; hereafter V12a), will show a near-infrared (NIR) and mid-infrared (MIR) excess due to a low-mass companion or due to interstellar and/or circumstellar material. The UV-excess catalogue of V12a consists of a mix of different populations, such as white dwarfs, interacting white dwarf binaries, subdwarfs of type O and B (sdO/sdB), emission line stars and QSOs. Due to the limited statistics and inhomogeneity, the fraction of optically selected white dwarfs with an IR-excess due to a low-mass companion is very uncertain in the Galactic Plane (Hoard et al., 2011). The UV-excess catalogue of V12a offers a complete white dwarf sample for this purpose, eventhough the sample also contains other populations. A distinction between white dwarfs with a companion or disk and e.g. Young Stellar Objects (YSOs), Be stars and Cataclysmic Variables can be made using the strength of the Hα emission (Witham et al., 2008, Corradi et al., 2010, Barentsen et al., 2011). A fraction of the subdwarf stars and A-type stars in the UV-excess catalogue might show an IR-excess (Hales et al., 2009), and UV-excess sources can also have both an optical blueness and infrared-excess when they are non-stellar, e.g. QSOs (Roseboom et al., 2012, Xue-Bing et al., 2012, Wright et al., 2010).

The *UVEX* survey images a 10×185 degrees wide band ($-5°< b <+5°$) centered on the Galactic equator in the U, g, r and He I λ5875 bands down to $\sim 21^{st} - 22^{nd}$ magnitude using the Wide Field Camera mounted on the Isaac Newton Telescope on La Palma (Groot et al., 2009). From the first 211 square degrees of *UVEX* data a catalogue of 2 170 UV-excess sources was selected in V12a. These UV-excess candidates were selected from the $(U - g)$ versus $(g - r)$ colour-colour diagram and g versus $(U - g)$ and g versus $(g - r)$ colour-magnitude diagrams by an automated field-to-field selection algorithm. Less than ∼1% of these selected *UVEX* sources are known in the literature. Spectroscopic follow-up of 132 UV-excess candidates selected from *UVEX* , presented in Verbeek et al. (2012b; hereafter V12b), shows that most UV-excess candidates are indeed genuine UV-excess sources such as white dwarfs, subdwarfs and interacting white dwarf binaries.

In this work we present the IR photometry of the UV-excess sources in the *UVEX* catalogues of V12a. Our goals are i) to see what fraction of the hot white dwarfs have a companion (late MS or BD), ii) to see if we can use IR photometry to select non-white dwarfs from our UV-excess catalogue, and iii) to see if we can find any debris disks. In Sect. 2 the cross-matching of the full UV-excess catalogue with IR/red surveys is presented. In Sect. 3 hot UV-excess candidate white dwarfs with $(g - r)<0.2$ with an IR-excess are selected and classified by fitting grids of reddened DA+dM and sdO/sdB models to the optical and infrared photometry. The spectral types of companions later than M6 are determined from the IR-excess. From these results the fraction of hot white dwarfs with a low mass companion is derived. In Sect. 4 the matches of the UV-excess sources in the *WISE* data are presented, and additionally a list of candidate QSOs with $|b|<5°$ is selected. Finally in Sect. 5 we summarise and discuss the conclusions.

2 CROSS-MATCHING WITH IR SURVEYS: UKIDSS, 2MASS AND WISE

The UV-excess catalogue of V12a (2 170 sources) is cross-matched with different surveys that image (parts of) the Galactic Plane at red/infrared (IR) wavelengths. An overview of the cross-matching is given in Table 1. Note that the coverage of the Galactic Plane and the overlap with the *UVEX* fields of V12a is not complete for all surveys (see Sect. 5). The results of the cross-matching are shown in the colour-colour diagrams of Figs. 1 to 5, where the spectroscopically classified sources of V12b are labelled. The *UKIDSS* and *2MASS* colour-magnitude diagrams are shown in the Appendix. As expected, in particular the redder and brighter *UVEX* UV-excess sources have a larger fraction of IR matches, as can be seen in the *UVEX* colour-colour and colour-magnitude diagrams of Figs. 1 to 2. The different IR surveys and the number of matches with the full UV-excess catalogue of V12a are described below.

• The UKIRT InfraRed Deep Sky Survey (*UKIDSS* , Lawrence et al., 2007) is a near-infrared survey imaging the northern sky in the J, H and K (1.2, 1.6 and 2.2 micron) filters using the Wide Field Camera (WFCAM) mounted on the 3.8m United Kingdom Infra-red Telescope (UKIRT) on Hawaii. The *UKIDSS* Galactic Plane Survey (*UKIDSS* GPS, Lucas et al., 2008, Lawrence et al., 2012) images the northern Galactic Plane in the same Galactic

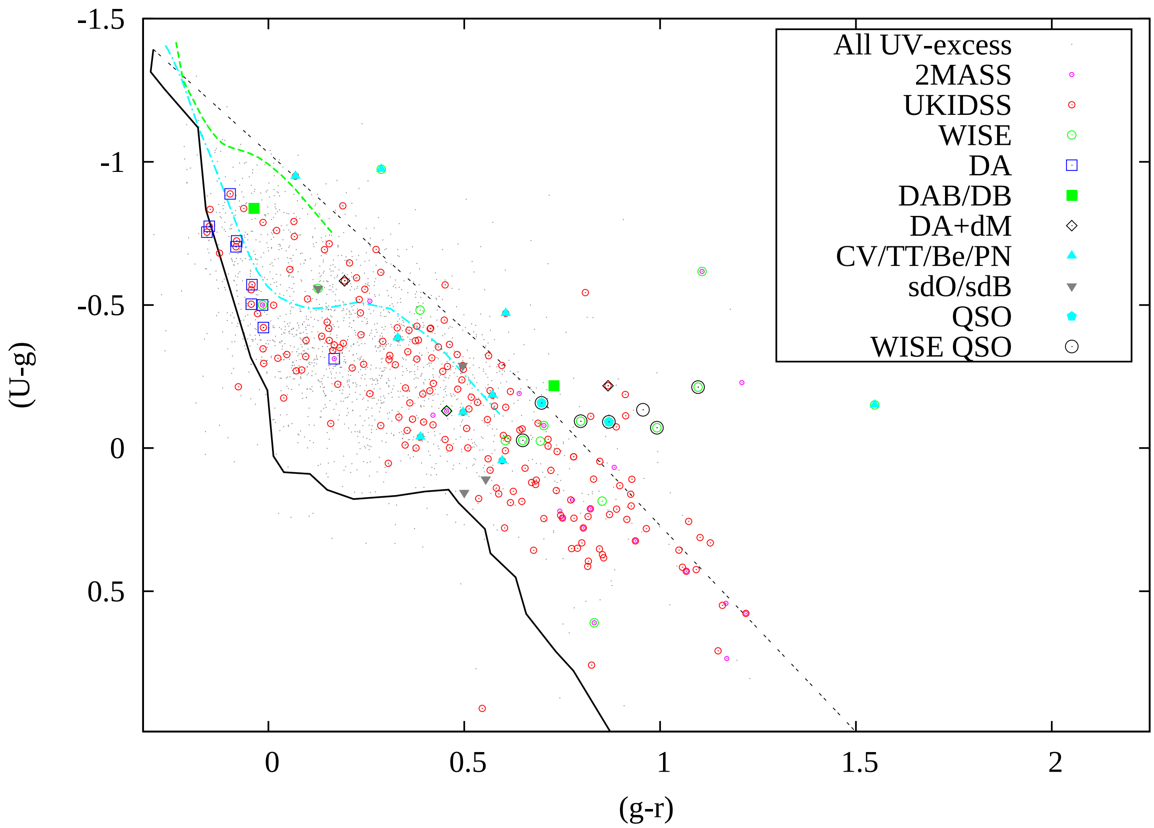

Figure 1. Colour-colour diagram with the UV-excess matches in UKIDSS, 2MASS and WISE. UV-excess sources spectroscopically classified in V12b are overplotted with different symbols. The lines are the simulated colours of unreddened main-sequence stars (solid black) and the O5V-reddening line (dashed black) of V12a. The cyan and green dashed lines are respectively the simulated colours of unreddened Koester DA and DB white dwarfs. The grey dots are the sources from the complete UV-excess catalogue of V12a.

Table 1. Summary of the cross-matching: No of matches with the full UV-excess catalogue and No of matches in the Deacon PM/Witham Hα catalogues (Deacon et al., 2009, Witham et al., 2008).

Catalogue:	Full UV-excess	PM/Hα
UKIDSS-GPS	227	4/6
2MASS	60	2/5
WISE	19	1/2
IPHAS-IDR	1 203	26/15
SDSS DR8	378	6/3

latitude range as *UVEX* and *IPHAS* . There is a match for a total of 227 UV-excess sources in all three *UKIDSS* filters within a radius of 1 arcsec (10% of the complete UV-excess catalogue). Note that the overlap of the *UKIDSS* GPS DR1 with the *UVEX* fields of V12a is not complete. The UV-excess 3-filter matches in *UKIDSS* with K>11 are plotted in the colour-colour diagram of Fig. 3 on top of the simulated unreddened main-sequence colours (Hewett et al., 2006). Of these *UKIDSS* matches there are 18 sources spectroscopically classified in V12b, 4 matches are in the IPHAS-POSSI proper motion catalogue (Deacon et al., 2009) and 6 matches are in the Hα emitter catalogue (Witham et al., 2008).

• The Two-Micron All-Sky Survey (2*MASS* , Skrutskie et al., 2006, Cutri et al., 2003) imaged the entire sky in the three near-infrared filter bands J, H and K (1.2, 1.7 and 2.2 micron) with a limiting magnitude of J=17.1, H=16.4 and K=15.3, using 2 automated 1.3m telescopes, one at Mt. Hopkins, Arizona, and one at CTIO, Chile. The overlap of the 2*MASS* All-Sky Catalog of Point Sources (Cutri et al., 2003) data and the *UVEX* fields of V12a is 100%. In 2*MASS* there is a match for 60 sources of the complete UV-excess catalogue in all three 2*MASS* filter bands within a radius of 1 arcsec (3%). Eighteen of these matches were spectroscopically classified in V12b, 2 matches are the IPHAS-POSS catalogue (1 classified as DA+dM) and 5 matches are in the Hα emitter catalogue (3 classified as T Tauri, Be star and Cataclysmic Variable). The UV-excess matches in 2*MASS* are plotted in the colour-colour diagram of Fig. 4.

• The Wide-field Infrared Survey Explorer (*WISE* , Wright et al., 2010) mapped the sky at four mid-infrared bands at 3.4, 4.6, 12, and 22 micron ($W1$, $W2$, $W3$ and $W4$). The overlap of the *WISE* All-Sky Data Release (Cutri et al., 2012) and the *UVEX* fields of V12a is 100%. The *WISE* data are used to select and classify UV-excess sources with a mid-IR excess, and a list of UV-excess candidate QSOs is selected in Sect. 4. There is a match for

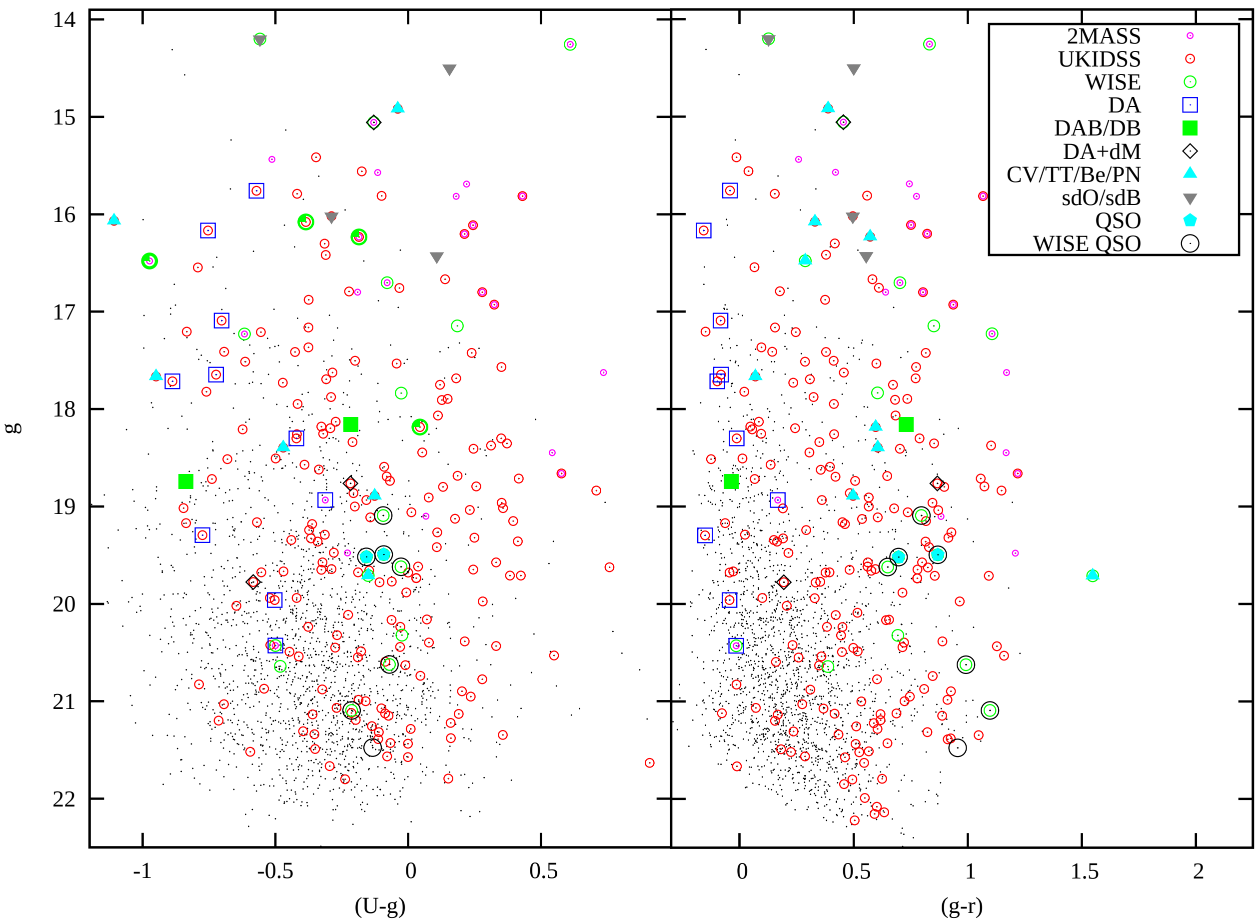

Figure 2. Colour-magnitude diagrams with the UV-excess matches in UKIDSS, 2MASS and WISE. Spectroscopically identified UV-excess sources of V12b are overplotted with different symbols. The grey dots are the sources from the complete UV-excess catalogue of V12a.

20 UV-excess sources in *WISE* within a radius of 1 arcsec in at least the first three filters (W1, W2, W3). Thirteen of them have a match in all four *WISE* filters. The 3-filter matches are shown in the colour-colour diagram of Fig. 5.

• The INT/WFC Photometric Hα Survey of the Northern Galactic Plane (*IPHAS* , Drew et al., 2005) has imaged the same survey area as *UVEX* with the same telescope and camera set-up using the r, i and $H\alpha$ filters. There is a match for 1 203 of our 2 170 UV-excess sources in the *IPHAS* initial data release (IDR, González-Solares et al., 2008) within a radius of 1.0 arcsec (55%). Note that the overlap of the *IPHAS* IDR with the *UVEX* fields of V12a is not complete, but ∼90%. The result of the cross-match between the UV-excess catalogue and *IPHAS* IDR was already shown in Figs. 10 and 11 of V12a and Fig. 3 of V12b. If available, the *IPHAS* data is used to distinguish UV-excess white dwarfs from UV-excess sources showing Hα emission, and the i-band photometry is used in the spectral fitting in Sect. 3.2. In the colour-colour diagrams of Figs. 3 to 5 the sources that are in the *IPHAS* Hα emitter catalogue (Witham et al., 2008) or IPHAS-POSS proper motion (PM) catalogue (Deacon et al., 2009) are circled red and blue respectively. The Witham Hα emitter catalogue covers the magnitude range $13<r<19.5$ and the Deacon IPHAS-POSS PM catalogue covers the magnitude range $13.5<r<19$. Matches in the Hα emission line star catalogue are expected to be Galactic sources, except for QSOs with redshift 0.5 or 1.3, which have emission lines exactly in the bandpass of the *IPHAS* Hα filter (Scaringi et al., 2013).

• Additionally, the Sloan Digital Sky Survey (*SDSS* , York et al., 2000) Photometric Catalog DR 8 (Adelman-McCarthy et al., 2011) overlaps with some *UVEX* Galactic

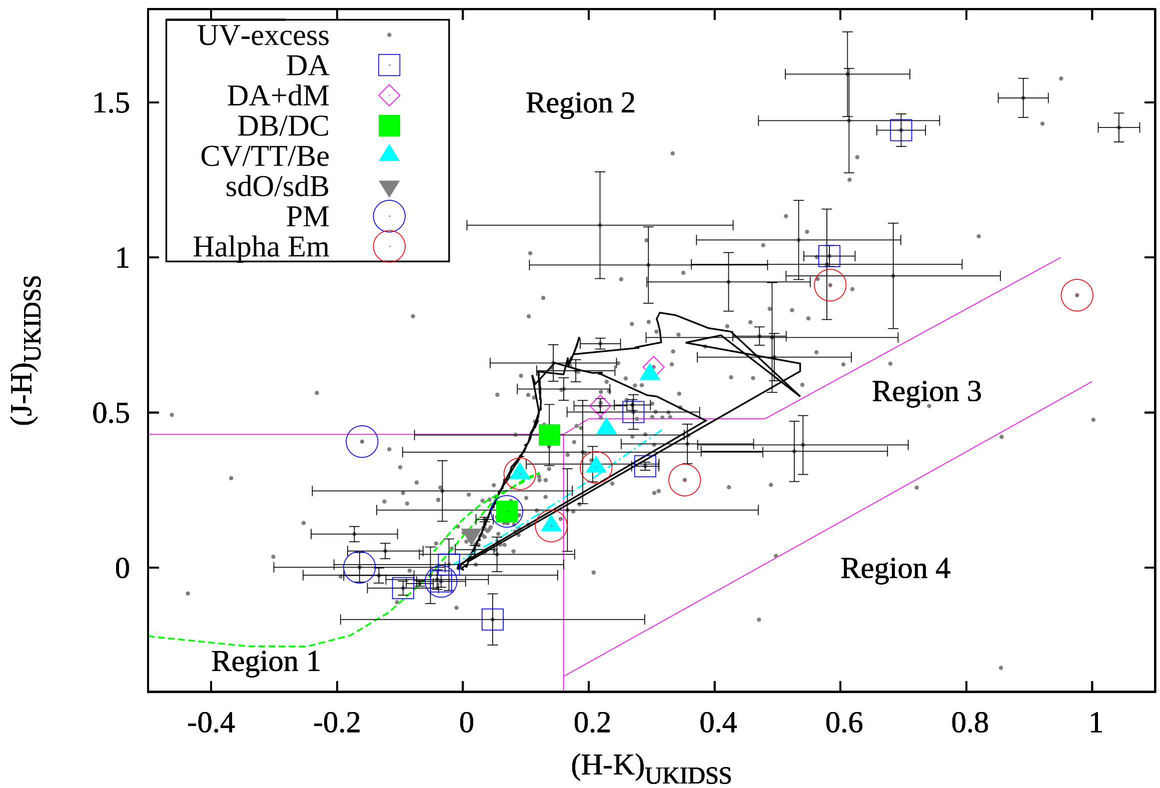

Figure 3. The $(J-H)$ vs. $(H-K)$ colour-colour diagram with the UKIDSS-GPS matches. The tracks are the unreddened UKIDSS colours of main-sequence stars (black), DA white dwarfs (green) and DB white dwarfs (cyan). UV-excess sources spectroscopically classified in V12b are overplotted with different symbols, UV-excess candidate white dwarfs with $(g-r)$ <0.2 are plotted with error bars, other UV-excess sources are plotted with dots. The four regions are indicated that contain different candidates: 1) single white dwarfs, 2) white dwarfs with an M-dwarf companion, 3) candidate white dwarfs with a later type (brown dwarf) companion, and 4) white dwarf with circumstellar material or a debris disk.

Plane fields. *SDSS* images the sky in the filters u, g, r, i, z down to $\sim 22^{nd}$ magnitude, using the 2.5m wide-angle optical telescope at Apache Point Observatory, New Mexico, US. For the full UV-excess catalogue 378 sources have a match in *SDSS* within a radius of 1 arcsec. Note that the overlap between *SDSS* and the *UVEX* fields of V12a is not complete. There are 6 *SDSS* UV-excess matches in the IPHAS-POSS PM catalogue and 3 *SDSS* UV-excess matches are in the *IPHAS* Hα emitter catalogue. For the UV-excess sources that have an *SDSS* match, the additional i-band and z-band photometry is used for the spectral fitting (Fig. 1, Rebassa-Mansergas et al., 2012) in Sect. 3.2.

3 CANDIDATE WHITE DWARFS WITH AN INFRARED COUNTERPART

The UV-excess catalogue consists of a mix of different populations. From the spectroscopic follow-up of V12b, 52% of the UV-excess sources are single DA white dwarfs, 14% are white dwarfs of other types (DAB/DB/DC/DZ/DAe), 4% are DA+dM white dwarfs, 11% are sdB/sdO stars, 9% are Hα emission line objects, 8% are BHB/MS stars and 2% are QSO. In Sects. 3.1 and 3.2 we focus in particular on hot white dwarfs with an IR-match. For that reason a sub-sample of 964 UV-excess candidate white dwarfs with $(g-r)$<0.2 is selected, which corresponds with the simulated unreddened colours of DA white dwarfs hotter than $T_{\rm eff}$>9 000K. This sub-sample does not contain DA white dwarfs cooler than $T_{\rm eff}$<9 000K or strongly reddened white dwarfs. From spectroscopic follow-up (Fig. 1, V12b) it is known that 97% of the DA white dwarfs identified in *UVEX* are in this colour range, but there will be ∼25% white dwarfs of other types and sdO/sdB stars which also may have infrared counterparts. Only the IR-matches of the sources from this UV-excess candidate white dwarf sub-sample are plotted with error bars in the colour-colour diagrams of Figs. 3 to 5.

3.1 Classification of white dwarfs in UKIDSS and 2MASS

In the hot sub-sample there are 46 UV-excess candidate white dwarfs with a *UKIDSS* match, and 3 with a 2*MASS* match. These matches are plotted with error bars in the colour-colour diagrams of Figs. 3 and 4. To separate single white dwarfs from white dwarfs with a companion or white dwarfs with a debris disk the $(J-H)$ vs. $(H-K)$

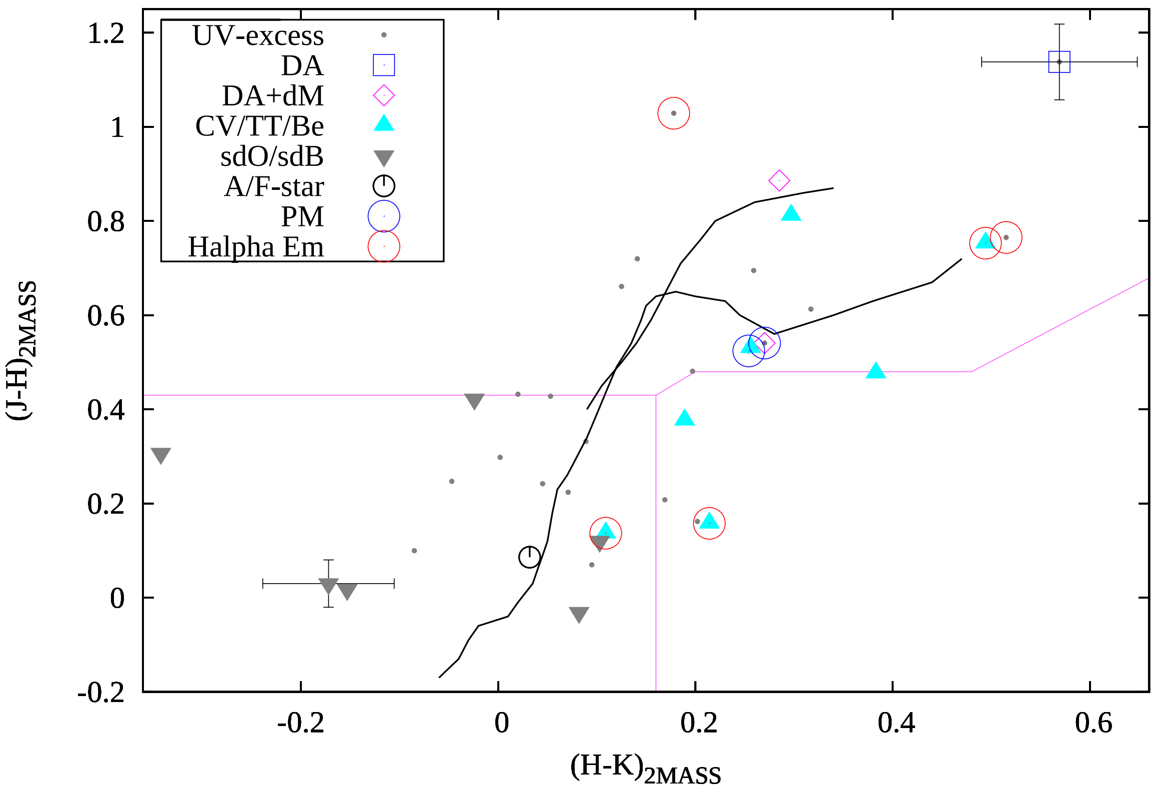

Figure 4. $(J-H)$ vs. $(H-K)$ colour-colour diagram with the UV-excess matches in 2MASS. The black lines are the simulated colours of main-sequence stars and giants with $E(B-V)$=0. Classified sources are labelled with different symbols, UV-excess candidate white dwarfs are plotted with error bars, other UV-excess sources are plotted with dots. There is one more match at $(H-K)$=1.15, $(J-H)$=2.6, classified as DA white dwarf in V12b, not visible in this figure.

colour-colour diagram is divided in four separate regions following Wachter et al. (2003) and Steele et al. (2011). The different regions in Fig. 3 contain different candidates:

- Region 1: There are 17 UV-excess sources that are single candidate white dwarfs, of which 4 were already classified as hydrogen atmosphere (DA) white dwarfs and 1 classified as sdB star in V12b.
- Region 2: Sources in region 2 are candidates for white dwarfs with an M-dwarf companion. There are 22 UV-excess candidates, of which 11 have g<20. Five of these sources are classified as single DA white dwarfs in V12b. However, the available spectra cannot exclude the presence of a late-type companion.
- Region 3: Sources in region 3 are candidates for white dwarfs with a later type (brown dwarf) companion. There are 7 UV-excess candidate white dwarfs, one of them is classified as a DA white dwarf in V12b (UVEXJ202659.21+411644.1). The available spectrum cannot exclude the presence of a very late-type companion.
- Region 4: Sources in region 4 show a K-band excess, possibly due to circumstellar material or a disk. There are 5 UV-excess sources, but none of them are candidate hot white dwarfs since they have $(g-r)$>0.2 in *UVEX* .

3.2 Determination of Spectral Types

For the UV-excess candidate white dwarfs with an IR-excess match in *UKIDSS* and/or *2MASS* the Spectral Energy Distributions (SEDs) are fitted in order to determine the spectral types. Grids of DA+dM model spectra, in the range $0<E(B-V)<1.0$ at $E(B-V)$=0.1 intervals, using the reddening laws of Cardelli, Clayton & Mathis (1989), are fitted to the optical and infrared photometry in order to determine white dwarf temperatures. For the fitting the white dwarf atmosphere models and M-dwarf models are both placed at the same distance. The spectral fluxes of Beuermann, 2006 are used to calibrate the absolue fluxes of the M-dwarfs. The grid of DA+dM model spectra is constructed from white dwarf atmosphere model spectra of Koester (2001) with $log\,g$=8.0 in the range $6\,000<T_{\rm eff}<80\,000$K, and template spectra of main-sequence stars from the library of Pickles (1998) with spectral type M0V to M6V. First, the *UVEX* photometry is used to determine the temperature of the white dwarf. For the DA+dM SED fitting the photometry of *UVEX* , *UKIDSS* and *2MASS* , and additionally if available, the *IPHAS* and/or *SDSS* photometry is used for 40 candidate white dwarfs. The *WISE* photometry is not used since the wavelength range of the DA+dM models only covers 3 000-25 000 Å, but consistency with the *WISE* photometry

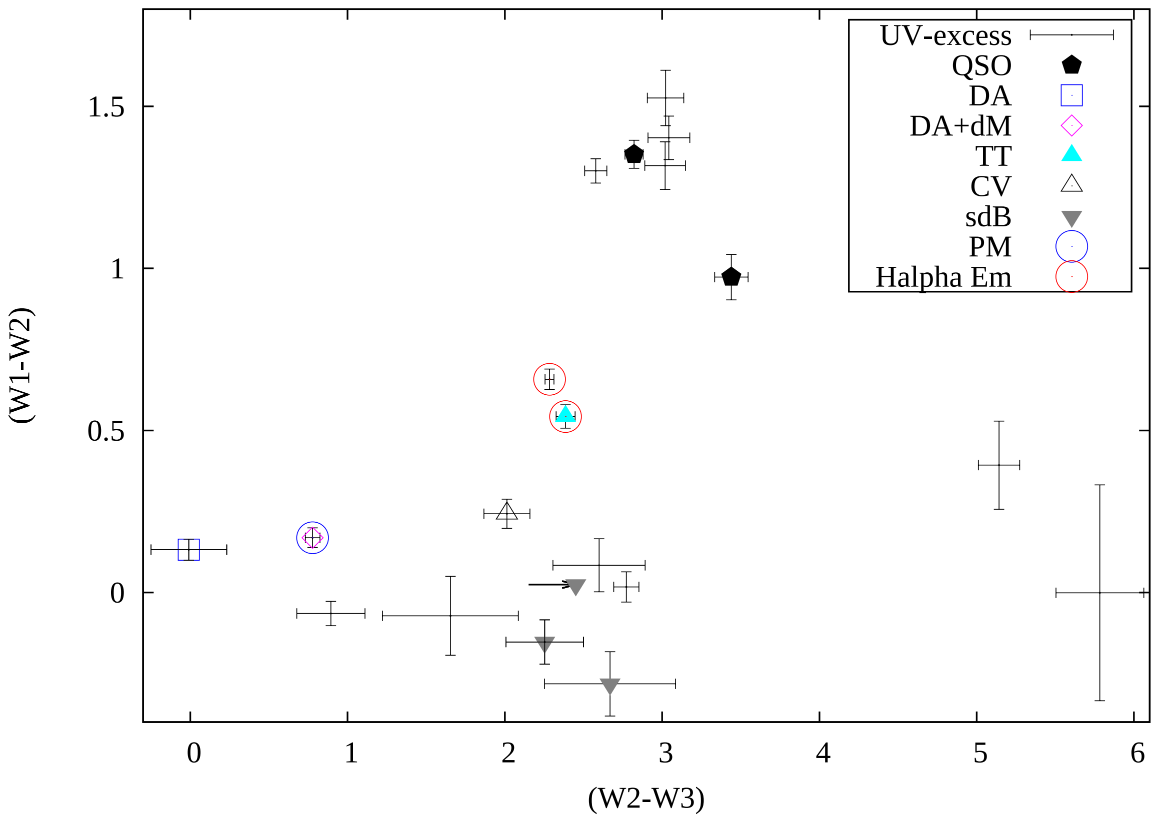

Figure 5. WISE matches within 1 arcsec plotted in the WISE colour-colour diagram. Sources which are classified from their spectra in V12b are overplotted with different symbols, all UV-excess matches are plotted with error bars. The 2 sources at $(W2-W3)$=0 and $(W2-W3)$=5.8 are UV-excess candidate white dwarfs with $(g-r)$ <0.2, 1 classified as DA white dwarf in V12b and 1 unclassified source with a strong $W3$ excess and $(W3-W4)$=2.1.

was checked, see e.g. Fig. 7.

The DA+dM models do not give a good fitting result for all candidate white dwarfs with an IR-excess match. Some UV-excess sources with an IR-excess match can be fully explained by a reddened sdB or sdO spectrum without any companion, or the IR-excess can be explained by an sdB/sdO stars with an F-, G- or K-type main-sequence companion. SdB/sdO stars with later companions can not be identified with the current photometry because the sdB/sdO dominates the SED out to the K-band. Grids of TheoSSA (Ringat, 2012) sdB/sdO models with $log\, g$=5.5 in the range 20 000<$T_{\rm eff}$<50 000K and 0<$E(B-V)$<5.0 at $T_{\rm eff}$=1 000K and $E(B-V)$=0.1 intervals are fitted to the optical and infrared photometry to determine $T_{\rm eff}$ and the reddening of the sdB/sdO stars. For the sdO/sdB stars with a possible main-sequence companion, a grid is constructed from the reddened sdB/sdO models and the template spectra of main-sequence stars from the library of Pickles (1998) with spectral types A5V to M5V. Also here the *WISE* photometry is not used, but consistency was checked, since the sdO/sdB+MS models cover the wavelength range 3 000-25 000 Å.

Candidate white dwarfs in region 3 of the IR colour-colour diagrams have companions with spectral types later than M6. The spectral types of these companions are determined using the $(J-K)$ colours resulting after subtracting the white dwarf flux as explained in Reid et al., 2001 and Leggett et al., 2002. The *UKIDSS* colours are converted to AB colours taking into account the correction $(J-K)$=0.962 of Hewett et al. (2006).

In the original UV-excess catalogue there might be a possible systematic shift in the *UVEX* U-band data, which would influence the result of Spectral Energy Distributions fitting in this paper. For that reason recalibrated *UVEX* data, as explained in Greiss et al. (2012), is used. The shift in the original *UVEX* data does not influence the content of the UV-excess catalogue because the selection in V12a was done relative to the reddened main-sequence population. The magnitudes and colours of the UV-excess sources might still show a small scatter, similar to the early *IPHAS* data (Drew et al., 2005), since a global photometric calibration is not applied to the *UVEX* data.

To convert the magnitudes into fluxes (F) we use: $F = 10^{-0.4\times(mag_{(AB)}+48.6)}$ for *EGAPS* and *SDSS*. For *EGAPS* photometry the AB offsets U=0.927, g=-0.103, r=0.164 and i=0.413 need to be added to convert to AB magnitudes (González-Solares et al., 2008; Blanton & Roweis, 2007 and Hewett et al., 2006). To convert

UKIDSS photometry to AB magnitudes the correction J=0.938, H=1.379 and K=1.900 need to be taken into account (Hewett et al., 2006). For 2*MASS* the flux is derived using $F = F_\nu - 0\,mag \times 10^{-0.4\times(mag_{(Vega)})}$, where $F_\nu - 0\,mag$ is 1594, 1024 and 666,7 (Jy) for J, H and K respectively (Cutri et al., 2003). The *WISE* photometry is converted into fluxes using $F = F_{\nu 0} \times 10^{-0.4\times mag_{(Vega)}}$, where $F_{\nu 0}$ is the the "Zero Magnitude Flux Density" for the *WISE* filter bands: $W1$=309.54, $W2$=171.787, $W3$=12.82, $W4$=9.26 (Jy) (Wright et al. 2010).

3.3 Fitting results

To test our photometric fitting routine first the method is applied to the UV-excess candidate white dwarfs that were spectroscopically classified in V12b. Note that the aim of the fitting is not to derive accurate temperatures, spectral types and reddening, but to classify the sources, and to confirm (or to rule out) the presence of a companion or disk. Fitting results for 7 UV-excess sources, spectroscopically classified in V12b, with an IR-excess or just an IR match, are shown in Figs. 6 to 12. For some of these sources there is also a match in *WISE* (see Sect. 3.4).

- The object UVEXJ1909+0213, classified as DA+dM objects in V12b, is shown in Fig. 6. This source has $(g-r)$=0.87, so it is not in the UV-excess candidate white dwarf sub-sample. The best-fit model consists of a white dwarf with $T_{\rm eff}$=14kK with an M4V companion. This source is in region 2 of the 2*MASS* colour-colour diagram of Fig. 4 and in region 2 of the *UKIDSS* colour-colour diagram of Fig. 3. Note that only the photometry was used for the fitting.
- The object UVEXJ2122+5526, also classified as DA+dM objects in V12b, is shown in Fig. 7. This source has $(g-r)$=0.47, so it is also not in the UV-excess candidate white dwarf sub-sample. The model that fits best consists of a white dwarf with $T_{\rm eff}$=20kK with an M3V companion, which is consistent up to the $W3$ *WISE* photometry. This source is in region 2 of the 2*MASS* colour-colour diagram of Fig. 4 and is plotted in the *WISE* colour-colour diagram of Fig. 5.
- The SED of UVEXJ2239+5857, classified as He-sdO in V12b, shows a decreasing flux in the IR which can be explained with a reddened sdB/sdO spectrum with $T_{\rm eff}$=50kK, $log\,g$=5.5 and $E(B-V)$=0.8, which is the model that fits best for this object, see Fig. 8.
- The SED of UVEXJ0421+4651, classified as sdB+F in V12b, can be explained by a single reddened sdB/sdO spectrum, but the combination of a sdB and a K5V spectrum gives a slightly better fit with $T_{\rm eff}$=50kK, $E(B-V)$=1.0, see Fig. 9. This source was classified as sdB+F in V12b due to the CaII lines present in the optical spectrum.
- The photometry of UVEXJ0328+5035, classified as a sdB star in V12b, can be fully explained by a reddened sdB spectrum with $T_{\rm eff}$=30kK, $log\,g$=5.5 and $E(B-V)$=0.4, see Fig. 10. However, this object is known to be a sdB+dM binary from its radial velocity (Kupfer et al., in prep.). No sign of the companion is seen in the SED.
- The SED fitting method finds a DA+dM as best solution for source UVEXJ2034+4110 (Fig. 11), classified as a DA white dwarf in V12b. The best-fit DA+dM model is a $T_{\rm eff}$=13kK DA white dwarf plus an M6V companion. The strong infrared-excess is due to a low-mass companion with spectral type L8 as determined from the $(J-K)$ colour. However, the contribution of an low-mass companion with spectral type L8 would be less luminous than in Fig. 11, so the white dwarf is probably at a larger distance compared to the brown dwarf. Additionally, the blue/optical images have a match within 0.1 arcsec, while there is an offset for the infrared images of 0.6 arcsec. The white dwarf and L8 brown dwarf are expected to be at different distances and not physically associated.
- The source UVEXJ2102+4750 in Fig. 12, classified as a DA white dwarf with $T_{\rm eff}$=13.3kK and $log(g)$=8.1 in V12b, shows an IR-excess. None of the DA+dM models fit the photometry well, making it candidate for having a companion with spectral type L5 as determined from the $(J-K)$ colour. This source was classified as a DA white dwarf in V12b since there is no sign of the companion in the optical spectrum, which is consistent with the IR-excess which increases for wavelengths larger than λ>8 000 Å.

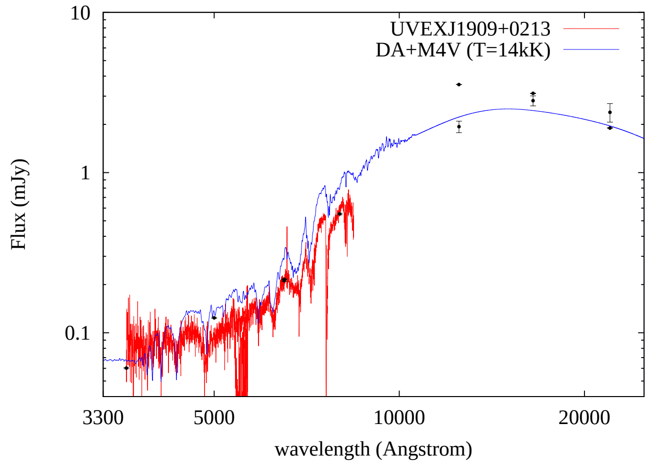

Figure 6. The SED of UVEXJ190912.34+021342.8, classified as DA+dM in V12b, with overplotted the best DA+dM model (blue), a $T_{\rm eff}$=14kK white dwarf plus M4V companion. Plotted here are the UVEX, IPHAS, 2MASS and UKIDSS photometry with error bars and the WHT spectrum of V12b (red).

The results of the fitting for all UV-excess candidate white dwarfs with an IR-excess match in *UKIDSS* and/or 2*MASS* are shown Table A1 of the Appendix A. Note that $T_{\rm eff}$ of the white dwarf and the spectral types of the companions are rough estimates, since only photometry is used for the fitting. From the positions in the $(J-H)$ vs. $(H-K)$ colour-colour diagram, and from the SED fitting, 24 UV-excess candidate white dwarfs are classified as white dwarf with an M-dwarf companion, 7 sources are candidate white dwarfs probably with a brown dwarf type companion (later than M-type), 19 UV-excess candidate white dwarfs are single white dwarfs or single sdO/sdB stars without a companion, and no UV-excess white dwarfs are clear debris disk candidates.

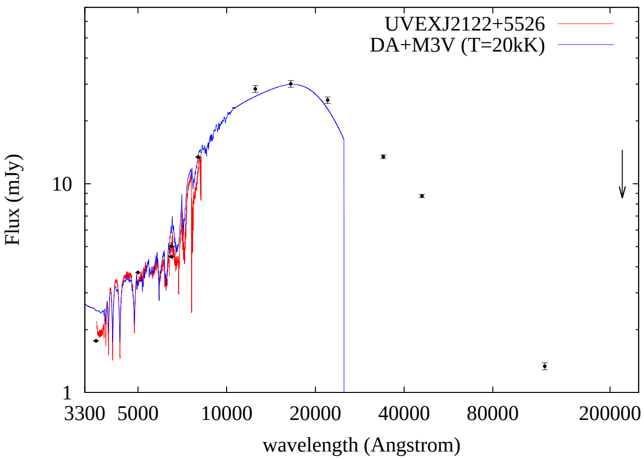

Figure 7. The SED of UVEXJ212257.82+552609.0, classified as DA+dM in V12b, can indeed be explained by DA+dM model (blue): a $T_{\rm eff}$=20kK white dwarf plus M3V companion, except for the W4 WISE photometry which is spurious. Plotted here are the UVEX, IPHAS, 2MASS and WISE photometry with error bars and the WHT spectrum of V12b (red).

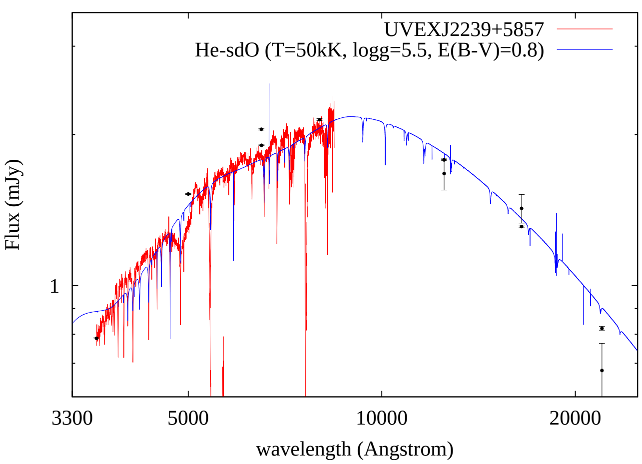

Figure 8. The photometry of UVEXJ223941.98+585729.1, classified as He-sdO in V12b, can be fully explained by a reddened He-sdO spectrum with $T_{\rm eff}$=50kK, $log(g)$=5.5 and $E(B-V)$=0.8 (blue). Plotted here are the UVEX, IPHAS, UKIDSS and 2MASS photometry with error bars and the WHT spectrum of V12b (red).

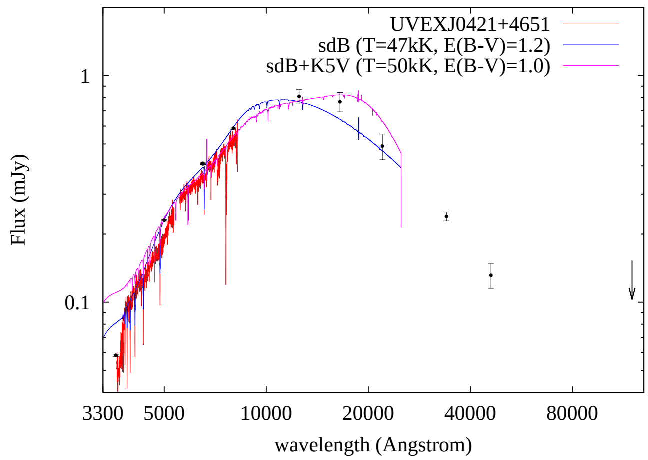

Figure 9. The photometry of UVEXJ042125.70+465115.4, classified as sdB+F in V12b, overplotted with a single sdB spectrum with $T_{\rm eff}$=47kK, $E(B-V)$=1.2 (blue), and the best-fit sdB+MS model: a sdB+K5V spectrum with $T_{\rm eff}$=50kK, $E(B-V)$=1.0 (magenta). Plotted here are the UVEX, IPHAS, 2MASS and WISE photometry with error bars and the WHT spectrum of V12b (red).

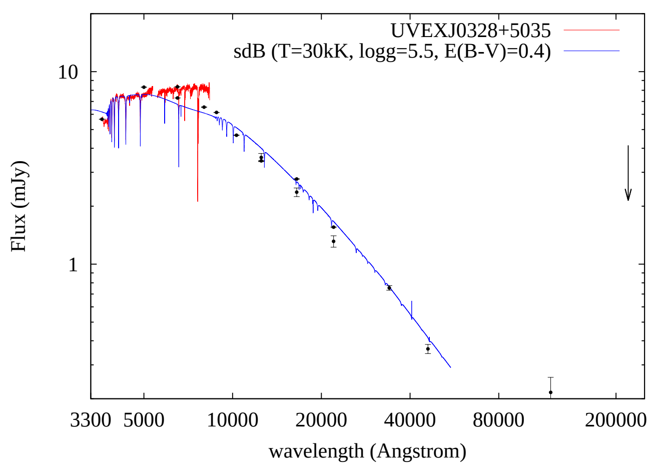

Figure 10. The photometry of UVEXJ032855.25+503529.8 can be fully explained by a reddened sdB model spectrum (blue) with $T_{\rm eff}$=30kK, $log(g)$=5.5 and $E(B-V)$=0.4. Plotted here are the UVEX, IPHAS, UKIDSS, 2MASS and WISE photometry with error bars and the WHT spectrum of V12b (red). The WHT spectrum might deviate at the red end of the spectrum ($\lambda >$7 500 Å) due to the flux calibration.

3.4 UV-excess sources in the Wide-field Infrared Survey data

The release of the all-sky *WISE* catalog (Cutri et al., 2012) contains all sky data in four mid-infrared bands centered at 3.4, 4.6, 12 and 22 micron. There are 9 classified UV-excess sources with a *WISE* match, 1 classified as DA white dwarf, 1 classified as Cataclysmic Variable, 1 classified as DA+dM, 1 classified as T Tauri star, 3 classified as sdB stars, and 2 classified as QSOs in V12b. The QSOs and 4 new QSO candidates are discussed in Sect. 4. The SEDs of the sources classified as DA+dM (UVEXJ2122+5526), DA (UVEXJ2034+4110; ccd-flag "H" for $W3$), sdB+F (UVEXJ0421+4651; $W3$ and $W4$ are upper limits), and sdB (UVEXJ0328+5035) in V12b, were already shown in Figs. 7 to 11. The SEDs of objects of other types, classified in V12b, with a match in *WISE* are shown in Fig. 13. The two unclassified UV-excess sources (UVEXJ2039+3647 and UVEXJ0009+6514) at $(W2-W3){\sim}5.5$ show a strong excess in the $W3$-band (UVEXJ0009+6514 has ccd-flag "H" in $W2$). From their SEDs and position in the *WISE* colour-colour diagram, these two sources are candidate Luminous InfraRed Galaxies (LIRGs)/star-burst Sbc (Fig. 12 of Wright et al., 2010). The four remaining sources are DA+dM or sdB/sdO+MS candidates.

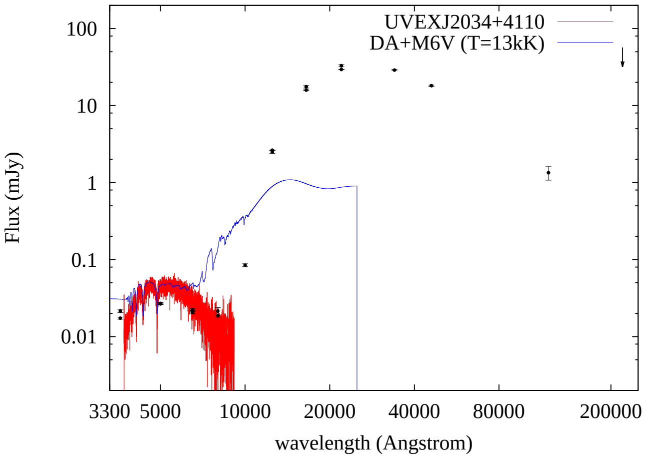

Figure 11. The SED of UVEXJ203411.72+411020.3, classified as single DA white dwarf in V12b, can not be explained by one of our DA white dwarf plus a late type companion models. The best-fit DA+dM model is a $T_{\rm eff}$=13kK white dwarf plus M6V companion (blue). The strong infrared-excess in 2MASS, UKIDSS and WISE can be explained by a later companion with spectral type L8. However, the contribution of this L8 dwarf is significantly more luminous than expected, so the WD and BD are expected to be at different distances and not physically associated. Plotted here are the UVEX, IPHAS, SDSS, 2MASS, UKIDSS and WISE photometry with error bars and the Hectospec spectrum of V12b (red).

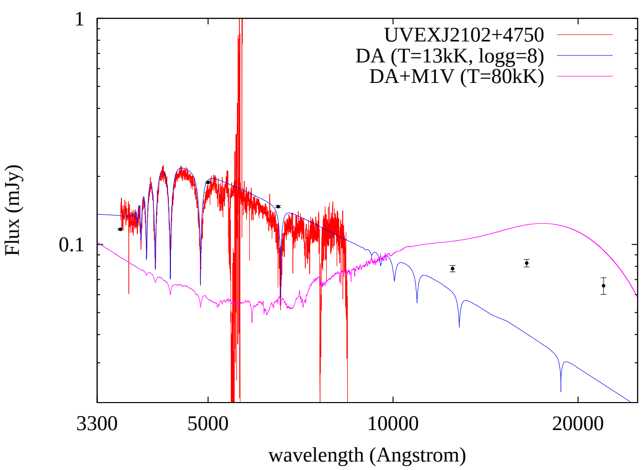

Figure 12. The SED of UVEXJ210248.44+475058.9, classified as DA white dwarf with $T_{\rm eff}$=13.3kK and $log(g)$=8.1 in V12b, shows a clear excess in the infrared which can be explained by a companion. The best-fit DA+dM model is a $T_{\rm eff}$=80kK white dwarf plus M1V companion (magenta), which is clearly too hot for the white dwarf. From the $(J-K)$ colour the spectral type of the companion is L5. Plotted here are the UVEX and UKIDSS photometry with error bars, the WHT spectrum of V12b (red) and a Koester DA white dwarf atmosphere model with $T_{\rm eff}$=13kK and $log(g)$=8.0 (blue).

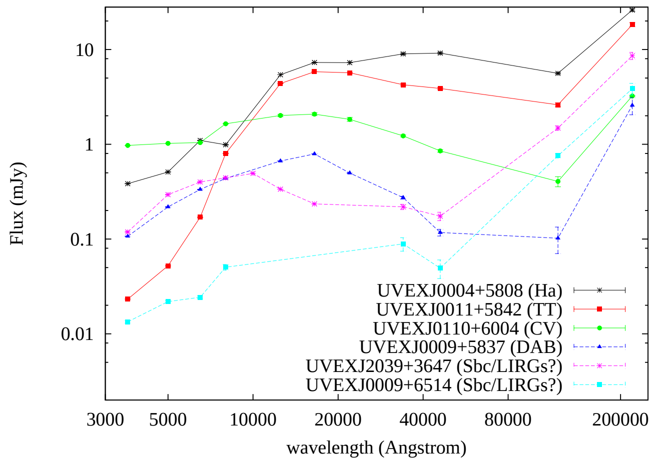

Figure 13. The SEDs of the UV-excess sources classified in V12b with a match in WISE and the 2 unclassified sources at $(W2-W3)$ ∼5.5 which are candidate star-burst Sbc/LIRGs (dashed lines).

4 CANDIDATE QSOS SELECTED FROM UVEX AND WISE

Since the release of the all-sky *WISE* catalog, the data have been used to select Quasi-Stellar Objects (QSOs, Bond et al., 2012, Stern et al., 2012, Xue-Bing Wu et al., 2012, Scaringi et al., 2012). The IR-excess of the QSOs in *WISE* is probably due to optically thick material surrounding most QSOs (Roseboom et al., 2012). In Fig. 5 there are 6 UV-excess sources at the QSO location in the *WISE* colour-colour diagram $(2.5<(W2-W3)<4.5$ and $0.6<(W1-W2)<1.7$, see Fig. 12 of Wright et al., 2010). Two of these sources (UVEXJ0008+5758 and UVEXJ0110+5829) were already spectroscopically classified as QSOs in V12b. For UVEXJ0110+5829 $W4$ is an upper limit, the other candidate QSOs have "good" photometry in all *WISE* bands. All 6 candidate QSOs have similar *UVEX* colours $(g-r)$∼0.8 and $(U-g)$∼–0.2. In V12a these 6 sources were selected in g vs. $(U-g)$ and not in g vs. $(g-r)$ (selection flags "515" and "514") and they are all at Galactic latitude $-5°<b<-4°$and Galactic longitude $117°>l>157°$. This might be due to the warp and flare of the Milky Way at this latitude and longitude (Cabrera-Lavers et al., 2007). The effects of the shape are different at different lines of sight, the height of the disk is smaller at some directions and therefore QSOs may be picked-up by UV-excess surveys. The two brightest candidate QSOs have a match in 2*MASS* , and 3 of the candidate QSOs have a match in *UKIDSS* . The SEDs of the 2 QSOs and new candidate QSOs are shown in Fig. 14. The characteristics of the 6 UV-excess candidate QSOs are summarized in Table 2.

5 DISCUSSION AND CONCLUSIONS

There are 46 white dwarfs with an infrared match in *UKIDSS* and 3 with a match in 2*MASS* . Seventeen sources in the $(g-r)<0.2$ sample turn out to be single white dwarfs. These white dwarfs have bright *UVEX* g-band

Table 2. UV-excess candidate QSOs from WISE

Name	l	b	Field	Selection	(r)	(g)	(U)	$W1$	$W2$	$W3$	$W4$
UVEXJ000848.64+575832.7	117.3	-4.43	48	515	18.625	19.494	19.402	14.189	12.837	10.016	8.126
UVEXJ033309.70+500541.8	147.6	-4.86	1243	515	18.296	19.093	18.999	13.642	12.341	9.763	7.532
UVEXJ033113.88+502156.9	147.2	-4.82	1243	515	19.996	21.093	20.880	15.637	14.111	11.089	8.817
UVEXJ022445.84+553325.9	135.9	-4.94	810	514	18.971	19.620	19.593	15.200	13.797	10.754	8.516
UVEXJ041204.47+444629.6	156.1	-4.80	1570	515	19.631	20.623	20.552	14.954	13.637	10.618	8.298
UVEXJ011037.91+582928.1	125.4	-4.29	404	515	18.821	19.518	19.360	15.056	14.083	10.643	8.262

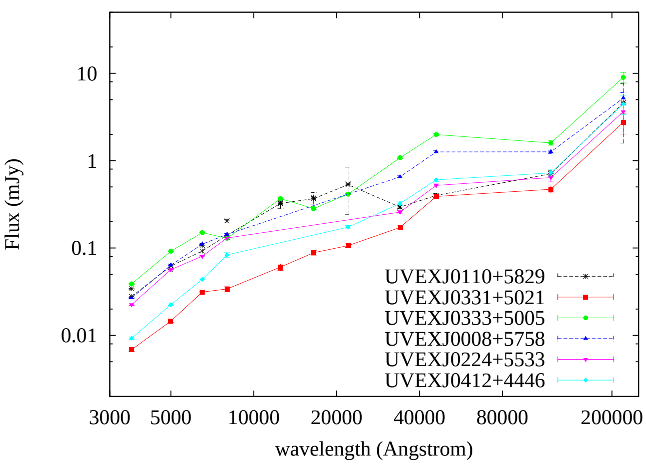

Figure 14. The SEDs of the 2 classified QSOs of V12b (dashed lines) and the 4 new candidate QSOs from WISE (solid lines).

magnitudes, have in general a higher $T_{\rm eff}$, and are more reddened compared to the candidate DA+dM sources in the UV-excess candidate white dwarf sample.

In the $(g-r)<0.2$ sample there are 24 DA+dM candidates, which is a fraction of 2% of the complete UV-excess candidate white dwarf sample. This fraction given here is a lower limit, since the fraction of white dwarfs with a companion is higher for the brighter UV-excess sources (see Figs. 1 to 2). If only UV-excess candidate white dwarfs brighter than $g<20$ are considered, the fraction of white dwarfs with a companion is 4%. If we compare this result to other studies, the DA+dM fraction is in the range 6-22% (Farihi, Becklin & Zuckerman, 2005; Debes, 2011). The presence of an M-dwarf has a strong influence on the optical colours for the cooler white dwarfs. Due to the contribution of the M-dwarf the colours of the most DA+dM sources are redder than $(g-r)>0.2$. An unreddened DA+M4V has $(g-r)=0.2$ for a $T_{\rm eff}\sim28$kK white dwarf (Fig. 1 of Rebassa-Mansergas et al., 2012; Fig. 2 of Augusteijn et al., 2008), while a single DA white dwarf with $T_{\rm eff}=28$kK is $(g-r)=-0.185$. The effects on the UV and optical spectrum due to the presence of a debris disks around white dwarfs is negligible (Zabot et al., 2009).

There are 7 candidates for white dwarfs with a companion later than type M6V in the UV-excess candidate white dwarf sample. These sources are all brighter than $g<20$ and the white dwarfs all have an effective temperature lower than $T_{\rm eff}<20$kK. This number is in agreement with the WD+BD fractions of other studies (Farihi, Becklin & Zuckerman, 2005; Debes, 2011).

No convincing debris disk candidates were found. If the expected rate of white dwarfs with a dust/debris disk would be ∼1% (Girven et al., 2011), there would be ∼4 of them brighter than g<20 in the UV-excess catalogue. Additionally, the IR-excess of one source (UVEXJ0328+5035) can be fully explained by a reddened sdB spectrum without the need for a low-mass companion.

There are 2 known QSOs and 4 UV-excess candidate QSOs in *WISE* . Since the number of QSOs from the *WISE* cross-matching (6 of 2 170) is much smaller than the fraction of QSOs found in the spectroscopic follow-up of UV-excess sources in V12b (2 of 132), there might be some more QSOs in the UV-excess catalogue. However, the QSOs at $|b|<5$ are expected to be clustered at specific lines of sight where absorption is not so strong. The fact that all known *UVEX* QSOs have a *WISE* match shows that adding *WISE* data is a good additional selection criteria. A list of UV-excess candidate QSOs is given in Table 2. The *UVEX* colours of these candidate QSOs are at $0.65<(g-r)<1.10$ and $-0.21<(U-g)<-0.03$ (Figs. 1 and 2), which are the colour ranges of known QSOs.

ACKNOWLEDGEMENT

This paper makes use of data collected at the Isaac Newton Telescope, operated on the island of La Palma by the Isaac Newton Group in the Spanish Observatorio del Roque de los Muchachos of the Instítuto de Astrofísica de Canarias. The observations were processed by the Cambridge Astronomy Survey Unit (CASU) at the Institute of Astronomy, University of Cambridge. Hectospec observations shown in this paper were obtained at the MMT Observatory, a joint facility of the University of Arizona and the Smithsonian Institution. We gratefully acknowledge the *IPHAS* consortium for making available the IPHAS-IDR data. The WHT/ISIS spectra were reduced in V12b using IRAF (Image Reduction and Analysis Facility). IRAF is distributed by the National Optical Astronomy Observatory, which is operated by the Association of Universities for Research in Astronomy (AURA) under cooperative agreement with the National Science Foundation. The authors would like to thank Detlev Koester for making available the white dwarf atmosphere model spectra. The TheoSSA service (http://dc.g-vo.org/theossa), used to retrieve theoretical sdO and sdB spectra for this paper, was constructed as part of the activities of the German Astrophysical Virtual Observatory. This research has made use of the Simbad database and the VizieR catalogue access tool, operated at CDS, Strasbourg, France. The original description of the VizieR service was published in A&AS 143, 23 This publication makes use of data products from the Wide-field Infrared Survey Explorer (*WISE*), which is a joint project of the University of California, Los Angeles, and the Jet Propulsion Laboratory/California Institute of Technology, funded by the National Aeronautics and Space Administration. This publication makes use of data products from the Two Micron All Sky Survey (2*MASS*), which is a joint project of the University of Massachusetts and the Infrared Processing and Analysis Center/California Institute of Technology, funded by the National Aeronautics and Space Administration and the National Science Foundation. This work is based in part on data obtained as part of the UKIRT Infrared Deep Sky Survey (*UKIDSS*). We want to credit the efforts of the teams which built WFCAM, processed the data, and implemented the *UKIDSS* surveys. The *UKIDSS* project is defined in Lawrence et al (2007). *UKIDSS* uses the UKIRT Wide Field Camera (WFCAM; Casali et al, 2007). The photometric system is described in Hewett et al (2006), and the calibration is described in Hodgkin et al. (2009). The pipeline processing and science archive are described in Irwin et al (in prep) and Hambly et al (2008). This paper uses data obtained by the Sloan Digital Sky Survey (*SDSS*) DR8 (Aihara et al. 2011a). The Sloan Digital Sky Survey III (Eisenstein et al. 2011) is an extension of the SDSS-I and II projects (York et al. 2000). It uses the dedicated 2.5-meter wide-field Sloan Foundation Telescope (Gunn et al. 2006) at Apache Point Observatory (APO). Funding for the Sloan Digital Sky Survey has been provided by the Alfred P. Sloan Foundation, the Participating Institutions, the National Aeronautics and Space Administration, the National Science Foundation, the U.S. Department of Energy, the Japanese Monbukagakusho, and the Max Planck Society. The *SDSS* Web site is *http://www.sdss.org/*. The *SDSS* is managed by the Astrophysical Research Consortium (ARC) for the Participating Institutions. KV is supported by a NWO-EW grant 614.000.601 to PJG and by NOVA.

REFERENCES

Adelman-McCarthy, J. K.; et al., 2011, yCat 2306, 0A
Aihara H., Allende Prieto C., An D., Anderson S.F. Aubourg E., Balbinot E., Beers T.C., et al., 2011, ApJS 193, 29A
Augusteijn T., Greimel R., van den Besselaar E.J.M., Groot P.J., Morales-Rueda L., 2008, A&A 486, 843A
Barber S.D., Patterson A.J., Kilic L., Leggett S.K., Dufour P., Bloom J.S., Starr D.L., 2012, ApJ 760, 26
Barentsen G., Vink J.S., Drew J.E., Greimel R. et al., 2011, MNRAS 415, 103B
Beuermann K, 2006, A&A 460, 783B
Blanton M.R. and Roweis S., 2007, AJ 133, 734B
Brinkworth C.S., Gänsicke B.T., Marsh T.R., Hoard D.W., Tappert C., 2009, ApJ 696, 1402B
Brinkworth C.S., Gänsicke B.T., Girven J.M., Hoard D.W., Marsh T.R., Parsons S.G., Koester D., 2012, ApJ 750, 86B
Cabrera-Lavers A., Bilir S., Ak S., Yaz E., Lopez-Corredoira M., 2007, A&A 464, 565C
Cardelli J.A., Clayton G.C. & Mathis J.S., 1989, ApJ 345, 245
Casali M., Adamson A., Alves de Oliveira C., Almaini O., Burch K., Chuter T., Elliot J. et al., 2007, A&A 467, 777C
Corradi R. L. M., Valentini M., Munari U., Drew J. E., et al., 2010, A&A 509, 41
Corradi R.L.M., Sabin L., Miszalski B., Rodrguez-Gil P., Santander-Garca M., Jones D., Drew J.E. et al., 2011, MNRAS 410, 1349C
Cutri R.M., Skrutskie M.F., van Dyk S. et al., 2003, yCat 2246, 0C
Cutri R.M. et al., 2012, yCat 2311, 0C
Deacon N.R., Groot P.J., Drew J.E., et al., 2009, MNRAS.397, 1685
Debes J.H., Hoard D.W., Wachter S., Leisawitz D.T., Cohen M., 2011, ApJS 197, 38D
Debes J.H., Walsh K.J., Stark C., 2012, ApJ 747, 148D
Debes J.H., Hoard D.W., Kilic M., Wachter S., Leisawitz D.T., Cohen M., Kirkpatrick J.D., Griffith R.L., 2011, ApJ 729, 4D
Debes J.H. & Sigurdsson, S., 2002, ApJ 572, 556D
Drew J.E., Greimel R., Irwin M., et al., 2005, MNRAS 362, 753 (D05)
Dufour P., Kilic M., Fontaine G., Bergeron P., Melis C., Bochanski J., 2012, ApJ 749, 6D
Eisenstein D.J., Weinberg D.H., Agol E., Aihara H., Allende Prieto C., Anderson S.F., Arns J.A., Aubourg, E., et al., 2011, AJ 142, 72E
Farihi J., Gänsicke B.T., Steele P.R., Girven J., Burleigh M.R., Breedt E., Koester D., 2012, MNRAS 421, 1635F
Farihi J., Becklin E.E. & Zuckerman B., 2005, ApJS 161, 394F
Gänsicke B.T., Koester D., Marsh T.R., Rebassa-Mansergas A., Southworth J., 2008, MNRAS 391L, 103G
Gänsicke, Boris T., 2011, AIPC 1331, 211G
Gänsicke B.T., Marsh T.R., Southworth J., 2007, MNRAS 380L, 35G
Gänsicke B.T., Koester D., Farihi J., Girven J., Parsons S.G., Breedt E., 2012, MNRAS 424, 333G
Girven J., Gänsicke B.T., Steeghs D. & Koester D., 2011, MNRAS 417, 1210G
González-Solares E.A., Walton N.A., Greimel R., Drew, J.E., et al., 2008, MNRAS 388, 89
Greiss S., Steeghs D., Gänsicke B.T., Martn E.L., Groot P.J. et al., 2012 AJ 144, 24G
Groot P.J., Verbeek K., Greimel R., et al., 2009, MNRAS 399, 323G
Gunn J.E., Siegmund W.A., Mannery E.J., Owen R.E., Hull C.L., Leger R.F, Carey L.N. et al., 2006, AJ 131, 2332G
Hales, A.S., Barlow M.J., Drew J.E., Unruh Y.C., Greimel R., Irwin M.J., Gonzlez-Solares E., 2009, ApJ 695, 75H
Hambly N.C., Collins R.S., Cross N.J.G., Mann R.G., Read M.A., Sutorius E.T.W., Bond I., Bryant J., et al., 2008, MNRAS 384, 637H
Heller R., Homeier D., Dreizler S., Oestensen R., 2009, yCat 34960191H
Hewett P.C., Warren S.J., Leggett S.K., Hodgkin S.T.,

2006, MNRAS 367, 454H
Hoard D.W., Debes J.H., Wachter S., Leisawitz D.T., Cohen M., 2011, AAS 21733309H
Hodgkin S.T., Irwin M.J., Hewett P.C. & Warren S.J., 2009, MNRAS 394, 675H
Jura M., 2003, ApJ 584L, 91J
Kilic M., Patterson A.J., Barber S., Leggett S.K., Dufour P., 2012, MNRAS 419L, 59K
Koester D., et al., 2001, A&A, 378, 556
Koester D., 2009, A&A 498,517K
Koester D. & Wilken D., 2006, A&A 453, 1051K
Lawrence A., Warren S.J., Almaini O., Edge A.C., Hambly N.C., Jameson R.F., Lucas P., Casali M., et al., 2007, MNRAS 379, 1599L
Lawrence A., Warren S.J., Almaini O., Edge A.C., Hambly N.C., Jameson R.F., Lucas P., Casali M., Adamson A., et al., 2012, yCat 2314, 0L
Leggett S.K., Golimowski D.A., Fan X., Geballe T.R., Knapp G.R., Brinkmann J. et al., 2002, ApJ 564, 452L
Lucas P. W., et al, 2008, 2008MNRAS.391..136L
Pickles A.J., 1998, PASP 110, 863
Rebassa-Mansergas A., Gänsicke B.T., Schreiber M.R., Koester D. and Rodríguez-Gil P., 2010, MNRAS 402, 620
Rebassa-Mansergas A., Nebot Gmez-Morn A., Schreiber M.R., Gänsicke B.T., Schwope A., Gallardo J., Koester D., 2012, MNRAS 419, 806R
Reid I.N., Burgasser A.J., Cruz K.L., Kirkpatrick J.D., Gizis J.E., 2001, AJ 121, 1710R
Ringat E., 2012, ASPC 452, 99R
Roseboom I.G., Lawrence A., Elvis M., Petty S., Shen Y., Hao H., 2012, arXiv 1205, 4543v2
Scaringi S., Groot P.J., Verbeek K., Greiss S., Knigge C. & Koerding E., 2013, MNRAS 428, 2207S
Silvestri N.M., Hawley S.L., West A.A., Szkody P., Bochanski J.J., Eisenstein D.J. et al., 2006, AJ 131, 1674S
Skrutskie M.F., Cutri R.M., Stiening R., Weinberg M.D., Schneider S., Carpenter J.M., Beichman C., Capps R., et al., 2006, AJ 131, 1163S
Steele P.R., Burleigh M.R., Dobbie P.D., Jameson R.F., Barstow M.A., Satterthwaite R.P., 2011, MNRAS 416, 2768S
Stern, D., Assef R.J., Benford D.J., Blain A., Cutri R., et al., 2012, ApJ 753, 30S
Verbeek K., Groot P.J., de Groot E., Scaringi S., Drew J.E., et al., 2012, MNRAS 420, 1115V
Verbeek K., Groot P.J., Scaringi S., Napiwotzki R., Spikings B., Østensen R.H., Drew J.E., Steeghs D. et al, 2012, MNRAS 426, 1235V
Wachter S., Hoard D.W., Hansen K.H., Wilcox R.E., Taylor H.M. & Finkelstein S.L., 2003, ApJ 586, 1356W
Wesson R., Barlow M., Corradi R., et al., 2008, ApJ 688, L21
Witham A.R., Knigge C., Drew J.E., et al., 2008, MNRAS 384, 1277
Wright N.J., Greimel R., Barlow M.J., Drew J.E., Cioni M.R.L., Zijlstra A.A. et al., 2008, MNRAS 390, 929W
Wright N.J., Drake J.J., Drew J.E. et al., 2012, ApJ 746L, 21W
Wu X.B., Hao G., Jia Z., Zhang Y. & Peng N., 2012, AJ 144, 49W
York D.G., Adelman J., Anderson J.E. et al., 2000, AJ 120,1579Y
Zabot A., Kanaan A., Cid Fernandes R., 2009, ApJ 704L, 93Z
Zuckerman B., & Becklin E E., 1987, Natur 330, 138Z

APPENDIX A: UV-EXCESS SOURCES WITH AN IR-EXCESS

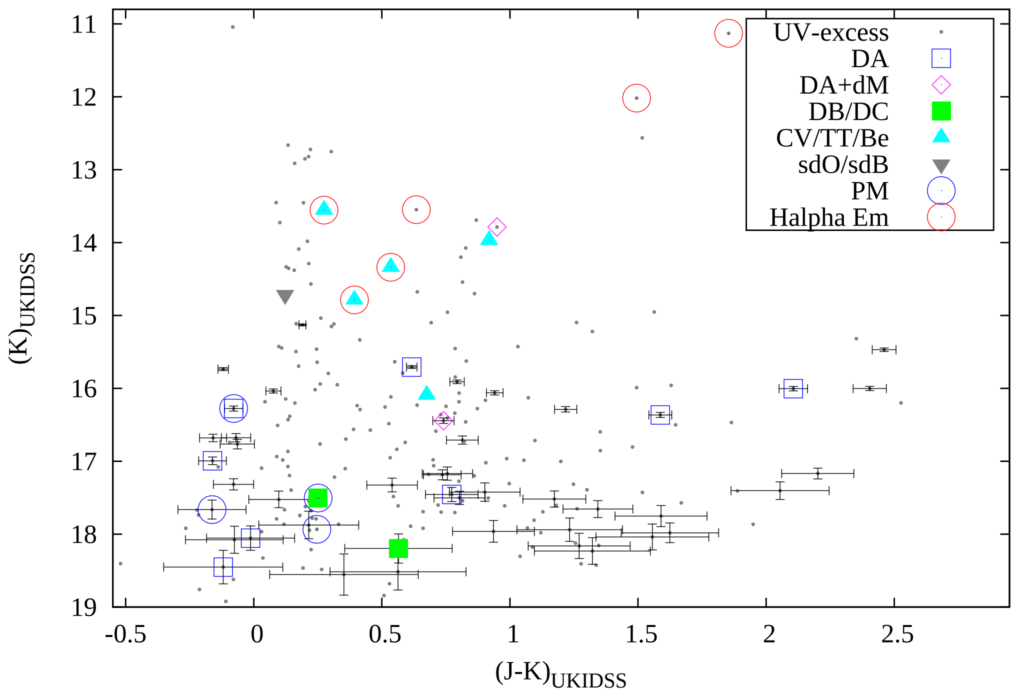

Figure A1. The K vs. $(J-K)$ colour-magnitude diagram with the UKIDSS-GPS matches. UV-excess sources spectroscopically classified in V12b are overplotted with different symbols, UV-excess candidate white dwarfs with $(g-r)$ <0.2 are plotted with error bars, other UV-excess sources are plotted with dots.

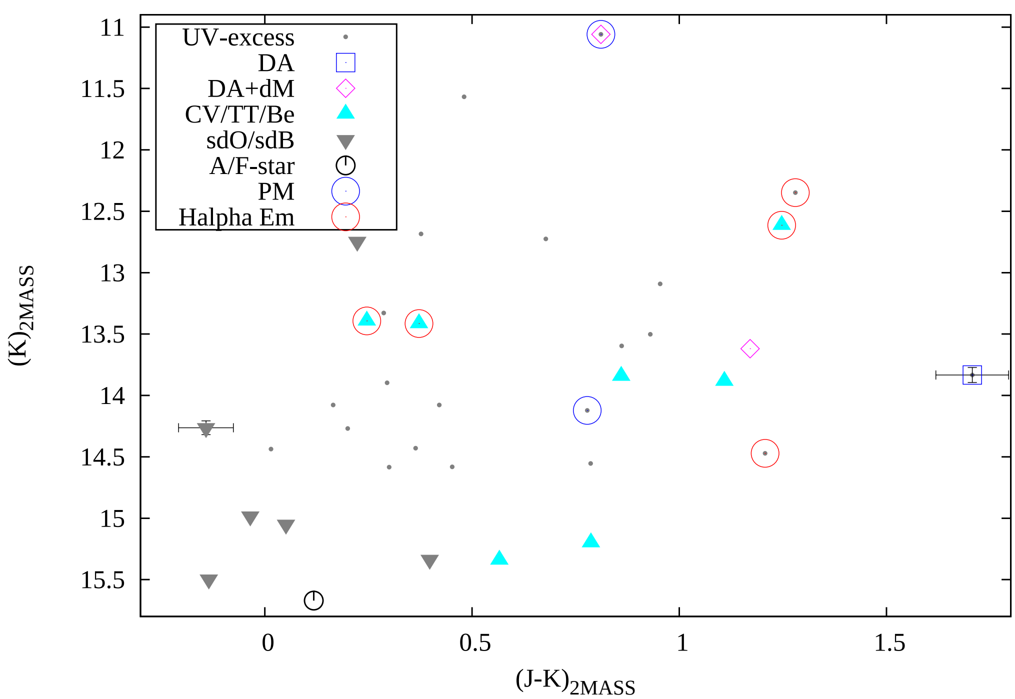

Figure A2. K vs. $(J-K)$ colour-magnitude diagram with the UV-excess matches in 2MASS. Classified sources are labelled with different symbols, UV-excess candidate white dwarfs are plotted with error bars, other UV-excess sources are plotted with dots. There is one more match at $(J-K)$=3.7, K=10.8, classified as DA white dwarf in V12b, not visible in this figure.

Table A1. UV-excess candidate white dwarfs with a match in UKIDSS (46) or 2MASS (3). Here “Selec” is column 20 of the UV-excess catalogue of V12a, “Reg.” is the region in the $(J-H)$ vs. $(H-K)$ colour-colour diagram, and “Fit” shows the fitting results: i) $T_{\rm eff}$ (kK) of the white dwarf, ii) $E(B-V)$, and iii) the spectral type of companion (M-type determined by fitting the photometry, or BD determined from the resulting $(J-K)$ colour).

No	Name	l	b	Field	Selec	r	g	U	(J)	(H)	(K)	Reg.	Fit	V12b
1	UVEXJ183141.67+002201.5	31.00431	4.55953	4088	1543	17.266	17.351	16.970	17.500	17.499	17.663	1	13,0.1	
2	UVEXJ183605.84+014117.8	32.68689	4.18264	4112	1028	18.651	18.717	17.978	17.922	17.346	17.186	2	22,0.2,M4V	
3	UVEXJ184610.80+022032.4	34.41846	2.23713	4183	1028	18.158	18.253	17.933	17.866	17.532	17.326	3	14,0.2,L2	
4	UVEXJ184725.16-011039.4	31.42575	0.35696	4197	1543	16.992	17.208	16.804	16.700	16.592	16.764	1	17,0.3	
5	UVEXJ184736.88-004413.1	31.84015	0.51452	4197	1543	20.435	20.594	20.508	19.457	18.016	17.403	2	13,0.3,M4V	
6	UVEXJ185519.35+114741.5	43.88889	4.49896	4294	1543	18.057	18.155	17.821	18.000	18.024	18.076	1	15,0.2	
7	UVEXJ185710.76+043917.5	37.72853	0.84714	4338	1543	19.266	19.290	18.976	17.930	16.512	15.469	2	22,0.1,M5V	
8	UVEXJ185941.43+013954.0	35.35485	-1.07596	4404	1543	18.133	18.180	17.853	18.325	17.949	17.423	3	13,0.1,L7	
9	UVEXJ190129.69+075854.1	41.17849	1.41266	4414	1543	17.800	17.815	17.046	18.089	17.842	17.874	1	24,0.2	
10	UVEXJ190257.79+113618.9	44.56953	2.74590	4469	1028	18.495	18.508	18.009	17.524	16.889	16.710	2	13,0.0,M6V	
11	UVEXJ190310.08+140658.9	46.83175	3.84480	4453	1028	17.595	17.667	16.743	17.621	17.578	17.524	1	35,0.3	
12	UVEXJ191001.10+055542.5	40.32597	-1.40915	4591	1543	18.154	18.209	17.585	17.926	17.526	17.170	3	20,0.2,L5	
13	UVEXJ202432.88+412338.9	79.33309	2.15868	5889	1543	17.351	17.207	16.286	17.835	18.387	19.690	1	22,0.0	
14	UVEXJ202654.69+430152.1	80.92379	2.74656	5923	1028	21.309	21.491	21.140	19.594	18.617	18.038	2	11,0.1,M6V	
15	UVEXJ202659.21+411644.1	79.50370	1.71848	5916	1028	17.175	17.092	16.389	16.323	15.996	15.707	3	17,0.0,L3	DA
16	UVEXJ202701.05+405909.2	79.26842	1.54359	5916	1028	20.996	21.067	20.797	19.607	18.666	17.982	2	14,0.2,M2V	
17	UVEXJ202800.47+405620.0	79.33903	1.36420	5939	1028	16.328	16.177	17.676	16.833	16.898	16.994	1	14,0.1	DA
18	UVEXJ202940.45+424613.7	81.00707	2.18354	5947	1028	19.839	19.939	19.418	17.505	16.758	16.287	2	50,0.2,M2V	
19	UVEXJ203238.52+411339.4	80.08644	0.82801	6010	1543	19.446	19.295	18.520	18.110	16.700	16.004	2	50,0.0,M6V	DA
20	UVEXJ203326.92+410959.9	80.12765	0.66975	6010	1543	20.967	21.135	20.775	18.406	16.892	16.001	2	13,0.1,M6V	
21	UVEXJ203614.30+392309.8	79.02005	-0.82249	6036	1029	19.582	19.776	19.192	17.184	16.662	16.443	2	45,0.4,M2V	DA+dM
22	UVEXJ204154.36+393201.4	79.80276	-1.60107	6118	1543	19.196	19.360	19.019	18.306	17.646	17.503	2	14,0.2,M4V	
23	UVEXJ204203.59+413343.1	81.42044	-0.37688	6112	1543	21.044	21.199	20.485	19.370	17.779	17.168	2	30,0.4,M0V	
24	UVEXJ204212.01+402706.7	80.56161	-1.08086	6111	1543	18.828	19.018	18.172	16.703	16.179	15.910	2	75,0.5,M6V	
25	UVEXJ204229.67+384058.0	79.20167	-2.21444	6108	1543	19.194	19.344	18.904	19.079	18.707	18.516	3	16,0.2,L2	
26	UVEXJ204401.03+403014.5	80.81605	-1.32043	6143	1543	15.436	15.419	15.044	15.616	15.667	15.736	1	14,0.1	
27	UVEXJ204502.52+414622.9	81.93084	-0.68385	6145	1543	17.255	17.406	16.741	17.238	17.276	17.317	1	28,0.4	
28	UVEXJ204502.62+385449.5	79.69073	-2.46193	6172	1028	21.678	21.666	21.370	19.553	18.449	18.231	2	30,0.1,M4V	
29	UVEXJ204503.63+435657.2	83.63666	0.66749	6153	1028	19.234	19.171	18.334	18.691	18.013	17.518	2	75,0.1,M5V	
30	UVEXJ204628.29+433237.6	83.47876	0.21540	6176	1543	20.841	20.827	20.039	18.999	18.078	17.656	2	20,0.1,M2V	
31	UVEXJ204720.64+444310.3	84.49330	0.82997	6196	1543	18.436	18.572	18.181	17.001	16.279	16.061	2	15,0.2,M2V	
32	UVEXJ204751.27+442920.1	84.37091	0.61442	6196	1028	20.004	19.960	19.457	17.952	16.947	16.365	2	14,0.0,M6V	DA
33	UVEXJ204804.01+421720.8	82.68492	-0.79916	6209	1543	19.721	19.677	19.124	19.431	18.456	18.161	2	14,0.0,M6V	
34	UVEXJ204830.05+423250.4	82.93598	-0.69880	6188	1031	21.198	21.121	20.907	19.172	18.430	17.939	2	13,0.1,M0V	
35	UVEXJ204856.21+444455.0	84.69394	0.62843	6196	1028	18.638	18.513	17.832	18.898	18.502	17.962	3	16,0.0,L7	
36	UVEXJ204914.51+421623.0	82.80950	-0.97798	6209	1028	16.610	16.784	16.434	16.608	16.554	16.677	1	14,0.2	
37	UVEXJ204938.33+432018.0	83.68083	-0.36073	6199	1543	19.137	19.328	18.962	18.906	18.721	18.555	3	11,0.1,M8V	
38	UVEXJ205037.81+424618.9	83.35761	-0.85988	6220	1543	15.793	15.750	15.132	16.198	16.242	16.277	1	15,0.0	DA
39	UVEXJ205148.13+442408.8	84.75023	0.01441	6219	1028	17.806	17.707	16.905	18.333	18.499	18.452	1	18,0.0	DA
40	UVEXJ205636.98+434541.6	84.81618	-1.05975	6293	1028	19.694	19.666	19.196	19.342	18.285	17.752	2	13,0.0,M6V	
41	UVEXJ210112.02+452020.7	86.54346	-0.64434	6355	519	16.131	16.272	17.069	16.114	16.056	16.037	1	14,0.8	
42	UVEXJ210248.44+475058.9	88.60784	0.81096	6341	1543	18.313	18.300	17.879	18.228	17.726	17.456	2	80,0.1,L5	DA
43	UVEXJ210454.41+460041.9	87.47634	-0.68123	6365	1543	18.778	18.738	17.856	18.762	18.334	18.196	1	24,0.1	DB
44	UVEXJ223634.77+591907.8	106.47749	0.82554	7139	1028	17.752	17.675	16.937	18.041	18.032	18.054	1	17,0.0	DA
45	UVEXJ224338.89+550318.5	105.25732	-3.37032	7188	519	16.501	16.547	15.781	16.521	16.546	16.680	1	24,0.2	
46	UVEXJ224436.07+544812.6	105.25981	-3.65677	7188	518	15.640	15.780	15.359	15.319	15.163	15.129	1	16,0.2	
47	UVEXJ032855.25+503529.8	146.76969	-4.84547	1224	519	14.078	14.205	13.591	14.121	14.091	14.263	1	sdO/sdB	sdB
48	UVEXJ185740.07+075557.3	40.70227	2.23345	4346	1028	18.821	19.024	18.656	15.540	14.402	13.833	2	DA+M/L5	DA
49	UVEXJ203411.72+411020.3	80.21601	0.56034	6010	1543	20.446	20.426	19.875	14.512	11.915	10.767	2	DA+M/L8	DA